國 立 交 通 大 學

影像與生醫光電研究所

碩士論文

利用選擇性缺陷填補法使得氮化鎵磊晶層品質改善的研究

Study of GaN epilayer quality improvement using defect selective passivation technique

研 究 生：謝奇穎

指導教授：林建中 教授

中華民國一百年十月

利用選擇性缺陷填補法使得氮化鎵磊晶層品質改善的研究

Study of GaN epilayer quality improvement using defect selective passivation technique

研 究 生：謝奇穎 Student：Chi-Ying Hsieh
指導教授：林建中 教授 Advisor：Prof. Chien-Chung Lin

國立交通大學
影像與生醫光電研究所
碩士論文

A Thesis
Submitted to Institute of Imaging and Biomedical Photonics
College of Photonics
National Chiao Tung University
in partial Fulfillment of Requirements
for the Degree of Master
in
Institute of Imaging and Biomedical Photonics ,
October 2011
Hsinchu, Taiwan, Republic of China

中 華 民 國 一 百 年 十月

利用選擇性缺陷填補法使得氮化鎵磊晶層品質改善的研究

研究生:謝奇穎 **指導教授:林建中教授**

國立交通大學

影像與生醫光電研究所

中文摘要

近年來，在半導體元件中，三五族材料的寬能隙特性引起專注並扮演重要的角色。而在固態照明的應用中，氮化鎵材料的發光二極體吸引大家的目光。此外，氮化鎵材料的其他應用也廣為人知，例如：全彩發光二極體背光顯示器、白光發光二極體以及藍光雷射。而發光二極體亟需改善輸出光功率。為了製作高效率發光二極體，與高品質、低缺陷密度的氮化鎵磊晶層有關。過去，已經證實選擇性填補缺陷方法有效的減低缺陷密度並可提高發光二極體特性。在本論文中，我們利用旋轉塗佈將二氧化矽奈米小球填補於缺陷孔洞，簡單化選擇性缺陷填補方法且達到製作高效率發光二極體的目的。經由光激發光與電激發光的分析，證實此方法可以有效提高氮化鎵磊晶層品質。

Study of GaN epilayer quality improvement using defect selective passivation technique

Student：Chi-Ying Hsieh **Advisor：Prof. Chien-Chung Lin**

Institute of Imaging and Biomedical Photonics

National Chiao Tung University

Abstract

In recent decades, the III-nitrides become an interesting class of wide band-gap materials and play an important role in semiconductor devices. GaN-based light emitting devices have attracted great attention in last decade due to its importance in solid state lighting applications. The GaN-based device are full color LED displays, white LEDs and high capacity storage devices. However, GaN-LEDs still require further improvement of optical output power. To successfully fabricate high efficient LED depends on the high quality GaN epilayer with low defect density. In previous work, we demonstrated that the defect selective passivation method could reduce defect density and enhance LED performance. In this thesis, we simplify the process of defect selective passivation technique by spin-coating silica nanospheres on GaN surface to block the propagation of dislocations. Moreover, we apply defect selective passivation technique to fabricate high efficient LED. The analysis of photoluminescence, cathodoluminecence and electroluminescence show the crystal quality of GaN epilayer is improved.

Acknowledgements

充實的碩士班生活即將告一段落。由衷感謝林建中老師不辭辛勞的指導，使我突破許多瓶頸而獲得成果。也謝謝中研院程育人博士提供完善的研究環境，及提點論文研究方向。由於有林老師與程老師的教導，不論是課業或實驗，亦或是處世待人上的態度，都令我獲益良多，謝謝您們。

在做實驗的過程中，首先要感謝明華學長，帶領著我學習研究該有的態度。而在最艱難的階段，非常謝謝哲榮、世邦以及博閔學長的協助，使得樣品可以如期完成且達到目標。還要謝謝中研院的家揚、尚樺、玟君、善允、諮宜、印聰、士超以及林博實驗室的學長們的幫助。非常慶幸有著一群好朋友，陪我度過低潮與分享喜樂，謝謝同實驗室的威麟，一起去鬆餅屋吃吃的智偉；謝謝那一年我們一起住的室友，祐慶、培修和俊鴻，感謝你們的「照顧」。也謝謝交大台南校區的大家，豐富了我這兩年的生活。

最後，感謝家人當我永遠的後盾，使我生活沒有後顧之憂。爸媽，您辛苦了。也謝謝女朋友，璽雯，體諒這些分隔兩地的日子。謝謝你們幫助我完成碩士班學業。

Contents

中文摘要 Ⅰ
English Abstract Ⅱ
Acknowledgment Ⅲ
Contents Ⅳ
Table Captions Ⅵ
Figure Captions Ⅶ
Chapter 1 Introduction 1
1.1 Development of III-nitrides materials….....................1
1.2 Characteristics of Gallium Nitride (GaN)......................2
1.3 Motivation and other techniques....................3
1.4 Reference…...................6
Chapter 2 Theories....................8
2.1 The physical mechanisms for light emitting diodes....................8
2.1.1 Internal quantum efficiency & Non-radiative recombination center.............8
2.1.2 The limits of light extraction efficiency...........10
2.2 Key issues for realizing high efficiency LEDs....................12
2.2.1 Quality issues of GaN epitaxial layers....................12
2.2.2 Light extraction of GaN LEDs....................13
2.3 Wet etching....................14
2.3.1 Defect properties on GaN surface....................14
2.3.2 Etching process in molten KOH....................15
2.4 Reference....................22
Chapter 3 Fabrication and measurement systems....................25
3.1 Scanning electron microscopy (SEM)....................26
3.2 Cathodoluminescent spectroscopy (CL)....................27
3.3 Atomic Force Microscopy (AFM)....................28
3.4 Micro photoluminescence spectroscopy (μ-PL)....................30
3.5 Electroluminescence spectroscopy (EL)....................32
3.6 Reference....................33
Chapter 4 Result and discussion 34
4.1 Fabricate LED on the GaN epilayer of defect selective passivation....................34
4.2 Analysis of defect selective passivation process....................35
4-3 Analysis of DSP-LED performance....................39
4-3-1 Optical properties analysis of LED grown on DSP epilayer....................39
4-3-2 Optical properties analysis of LED grown on DSP epilayer....................40
4.4 Reference....................46

Chapter 5 Conclusion and future work..47

Table Captions

Table. 2.1 Various chemicals etch GaN……………………………………………………….17

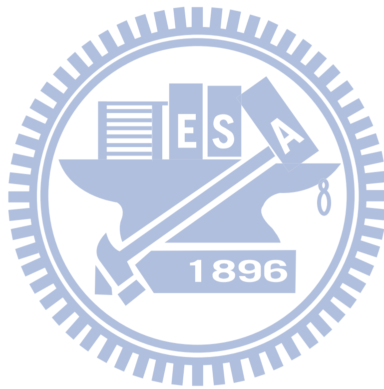

Figure Captions

Fig. 2.1 Schematic analogy carriers injected into active regions and depletion through radiative, onradiative, and leakage recombinations……………………………18
Fig. 2.2 Radiative and non-radiative recombination in active region………………………18
Fig. 2.3 (a) Cross section schematic diagram of typical LED structures……………………..19
Fig. 2.3 (b) Photon trajectories inside the LED………………………………………………19
Fig. 2.4 Total internal reflection in GaN-based LED…………………………………………19
Fig. 2.5 The angle of total internal reflection defines the light-escape cone…………………20
Fig. 2.6 (a) Illustration of Ga polarity (+c GaN, Ga-face)…………………………………...20
Fig. 2.6 (b) Illustration of N polarity (-c GaN, N-face)………………………………………20
Fig. 2.7 Schematic diagrams of the cross section GaN film viewed along [-1-120] direction for N-polar GaN to explain the mechanism of the polarity selective etching. (a) Nitrogen terminated layer with one negatively charged dangling bond on each nitrogen atom; (b) absorption of hydroxide ions; formation of oxides; (d) dissolving the oxides…………………………………………...............21
Fig. 3.1 Schematic diagram of a scanning electron microscope (SEM)……………………25
Fig. 3.2 Information that can be generated in the SEM by an electron beam striking the sample………………………………………………………………………………26
Fig. 3.3 JSM-7000F SEM and CL System……………………………………………………27
Fig. 3.4 (a) Contact mode of AFM……………………………………………………………29
Fig. 3.4 (b) Non-contact mode of AFM………………………………………………………29
Fig. 3.4 (c) Tapping mode of AFM……………………………………………………………29
Fig. 3.5 Interband transitions in photoluminescence system…………………………………31
Figs. 4.1[(a)-(d)] Schematic diagrams of defect selective passivation process……………36
Figs. 4.2[(a)-(c)] Schematic diagrams of simplified defect selective passivation process………………………………………………………………………………37
Fig. 4.3 Optical microscopy image of GaN surface etched at varied time and temperature…………………………………………………………...............37
Figs. 4.4[(a)-(b)] SEM image of GaN surface etched by H_3PO_4……………………………38
Figs. 4.5[(a)-(b)] SEM image of GaN surface etched by molten KOH………………………38
Figs. 4.6[(a),(b)] SEM image of GaN surface spin-coated nanospheres……………………38
Fig. 4.7 Photoluminescence spectrum…………………………………………………………39
Figs. 4.8[(a)-(c)] SEM and [(d)-(f)] CL cross section image of the defect selective passivatied epi-wafer under the same magnification…………………42
Figs. 4.9[(a)-(c)] Plane-view CL images of difference samples……………………………..43
Fig. 4.10 (a) CL spectrum of plane-view LED structure……………………………………..44
Fig. 4.10 (b) CL spectrum of cross section LED structure……………………………………..44

Fig. 4.11 L-I and V-I curve of DSP-LEDs and ref-LED…………………………………….......45
Fig. 4.12 Leakage current of DSP-LEDs and ref-LED under reverse bias…………………...45

Chapter 1 Introduction

1.1 Development of III-nitrides materials

Group of III-nitrides, aluminium nitride (AlN), gallium nitride (GaN) and indium nitride (InN), have been considered as a promising material for semiconductor devices applications since 1970, especially for the development of blue- and UV-light emitting diodes. Since last decade, the III-nitride becomes more and more important and find itself in a wide range of applications, [1-7] such as high-power transistors, high-frequency devices. InN and AlN can be alloyed with GaN. These wurtzite III-nitrides' direct band-gaps ranges from 0.7 eV for InN [8], to 3.4 eV for GaN, and to 6.2 eV for AlN [9]. In other words, the devices using III-nitrides could be activated at wavelength ranging from infrared to ultraviolet.

One important category of application is the GaN-based light emitting diode used for blue light, UV, and white (color-mixing) light LEDs; it allows high output power with small physical volume. When electricity is passed through GaN-based LEDs, the devices emit visible light. Generally, the emitted light is monochromatic and the advantages of the device include: low power requirement, high efficiency, and long lifetime.

1.2 Characteristics of Gallium Nitride (GaN)

GaN is a direct and wide band-gap semiconductor commonly used in bright light-emitting diodes since the 1990s. The compound is a very hard material that has a Wurtzite crystal structure. Its wide band gap (3.4eV) affords it special properties for applications in optoelectronics, high-power and high-frequency devices. For example, GaN is the substrate which makes violet (405 nm) laser diodes possible, without use of nonlinear optical frequency-doubling. Due to low sensitivity to ionizing radiation (like other group III nitrides), it is a suitable material for fabricating solar cell arrays for satellites. Moreover, GaN transistors can operate at hotter temperatures and work at much higher voltages than gallium arsenide (GaAs) transistors, they make ideal power amplifiers at microwave frequencies.

GaN is a mechanically stable material with large heat capacity. In its pure form it resists cracking and can be deposited in thin film on sapphire or silicon carbide, despite the mismatch in their lattice constants. GaN can be doped with silicon (Si) or with oxygen to n-type and with magnesium (Mg) to p-type; however, the doping atoms change the way the GaN crystals grow, introducing tensile stresses and making them brittle. GaN compounds also tend to have a high spatial defect frequency, on the order of a hundred million to ten billion defects per square centimeter.

High crystalline quality GaN has led to the commercialization of high-performance blue LEDs and long-lifetime violet-laser diodes, and to the development of GaN-based devices

such as UV detectors and high-speed field-effect transistors.

1.3 Motivation

Even though great progress has been made in the past few years, the GaN-based LED is still not as cost-effective as the traditional light source. One of the key issues is the low ouput power efficiency caused by defects or other problems during the epitaxial growth. In order to improve device performance, researchers are actively investigating various approaches. The overall performance of a LED can be decided by internal quantum efficiency and light extraction efficiency. The devices are often epitaxially grown on foreign substrates such as sapphire or silicon carbide (SiC) because a large-size commercial grade native substrate is still not available at a low cost. The as grown GaN epilayer has high threading dislocation (TD) density typically in the range of 10^8~10^{10} cm^{-2} owing to the mismatches in lattice constants and thermal expansion coefficients between GaN and sapphire. These defects are nonradiative recombination centers and are detrimental to optoelectronic device performance. For this reason, the reduction of TD is of great importance for the development of GaN based devices.

There are several epitaxial growth methods to improve crystal quality. A very commonly used one is the epitaxial lateral overgrowth technique (ELOG).[10,11] Strips of SiO_2 mask along specific crystal direction are deposited on GaN surface, followed by epitaxial growth.

The growth starts from the window regions and grows vertically as well as laterally to cover the SiO_2 strips until obtaining planar surface over whole wafer. The lateral growth above mask area bends the propagation direction of threading dislocation and results in significantly lower defect density. The defect density is, however, still high at window regions and coalescent boundaries. Another approach is to use patterned sapphire substrate for epitaxial growth,[12,13] but the reduction in TD defect density is often not as effective as ELOG method. Other methods use *in situ* SiN_x or *ex situ* TiN_x porous insertion layers,[14,15] where GaN nucleates from the pores of the inserted layer and lateral overgrowth on top of it. Recently, defect reduction methods using defect selective etching followed by metalorganic chemical vapor deposition (MOCVD)[16] or hydride vapor phase epitaxy[17] regrowth have also been reported.

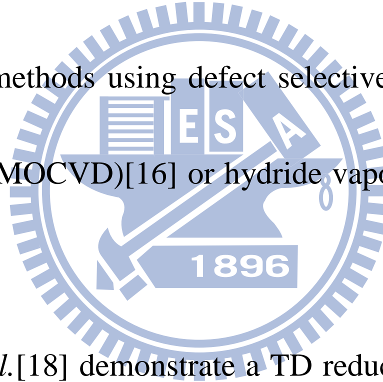

In previous letter, *Lo et al.*[18] demonstrate a TD reduction method by self-aligned defect selective passivation (DSP) without the need of photolithography and use it to fabricate a high efficiency light emitting diodes (LED). The defect selective passivation is done by defect selective etching, SiO_2 passivation at etch pits, and epitaxial over growth.

However, this technique requires complicated processes and expensive equipment such as depositing the SiO_2 thin film by PECVD and removing the SiO_2 film on GaN surface by chemical mechanical polishing. In this study, we demonstrate the use of silica nanospheres as a mask to block the propagation of TDs in GaN epitaxial layer growth. The process of

selective defect passivation by self-assembled silica nanospheres was performed through a simple spin-coating method and without photolithography patterning steps or expensive equipment. The proposed method has good potential to reduce the density of threading dislocations by blocking the propagation of TDs.

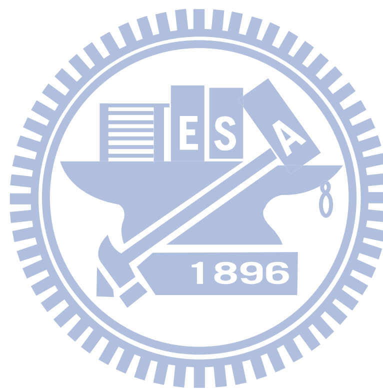

1.4 Reference

[1]. S. Nakamura, T. Mukai, and M. Senoh, *Appl. Phys. Lett.*, **67**, 1687 (1994)

[2]. S. Nakamura, M. Senoh, N. Iwasa, and S. Nagahama, Jpn. *J. Appl. Phys.*, **34**, L797 (1995)

[3]. G. Y. Xu, A. Salvador, W. Kim, Z. Fan, C. Lu, H. Tang, H. Markoc, G. Smith, M. Estes, B. Goldberg, W. Yank, and S. Krishnankutty, *Appl. Phys. Lett.*, **71**, 2154 (1997)

[4]. T. G. Zhu, D. J. H. Lambert, B. S. Shelton, M. N. Wong, U. Chowdhury, H. K. Kwon, and R. D. Dupuis, Electron Lett., 36, 1971 (2000)

[5]. G. T. Dang, A. P. Zhang, F. Ren, X. A. Cao, S. J. Pearton, H. Cho, J. Han, J. I. Chyi, C. M. Lee, C. C. Chuo, S. N. G. Chu, and R. G. Wilson, IEEE Trans. Electron Devices, 47, 692 (2000)

[6]. B. S. Shelton, D. J. H. Lambert, H. J. Jang, M. M. Wong, U. Chowdhury, Z. T. Gang, H. K. Kwon, Z. Liliental-Weber, M. Benarama, M. Feng, and R. D. Dupuis, IEEE Trans. Electron Devices, 48, 490 (2001)

[7]. A. P. Zhang, J. Han, F. Ren, K. E. Waldrio, C. R. Abernathy, B. Luo, G. Dang, J. W. Johnson, K. P. Lee, and S. J. Pearton, Electronchem. Solid-State Lett., 4, G39 (2001)

[8]. T. Matsuoka, H. Okamoto, M. Nakao, H. Harima, and E. Kurimoto, Appl. Phys. Lett., 81, 1246 (2002)

[9]. H. Morkoc, Nitride Semiconductors and devices, (Springer-Verlag, Berlin, 1999) [10] T.

Mukai, K. Takekawa, and S. Nakamura, Jpn. J. Appl. Phys., Part 2 **37**, L839 (1998).

[11] O.-H. Nam, M. D. Bremser, T. S. Zheleva, and R. F. Davis, Appl. Phys. Lett. **71**, 2638 (1997).

[12] E.-H. Park, J. Jang, S. Gupta, I. Ferguson, C.-H. Kim, S.-K. Jeon, and J.-S.Park, Appl. Phys. Lett. **93**, 191103 (2008).

[13] Y. J. Lee, H. C. Kuo, T. C. Lu, B. J. Su, and S. C. Wang, J.Electrochem. Soc. **153**, G1106 (2006).

[14] J. Xie, Ü. Özgür, Y. Fu, X. Ni, H. Morkoç, C. K. Inoki, T. S. Kuan, J. V. Foreman, and H. O. Everitt, Appl. Phys. Lett. **90**, 041107 (2007).

[15] Ü. Özgür, Y. Fu, Y. T. Moon, F. Yun, H. Morkoç, H. O. Everitt, S. S. Park, and K. Y. Lee, Appl. Phys. Lett. **86**, 232106 (2005).

[16] J. W. Lee, C. Sone, Y. Park, S.-N. Lee, J.-H. Ryou, R. D. Dupuis, C.-H. Hong, and H. Kim, Appl. Phys. Lett. **95**, 011108 (2009).

[17] J. L. Weyher, H. Ashraf, and P. R. Hageman, Appl. Phys. Lett. **95**, 031913(2009).

[18] M. H. Lo, P. M. Tu, C. H. Wang, Y. J. Cheng, C. W. Hung, S. C. Hsu, H. C. Kuo, H. W. Zan, S. C. Wang, C. Y. Chang, et al., *Appl. Phys. Lett.* **95**, 211103 (2009)

Chapter 2 Theories

2.1 The physical mechanisms for light emitting diodes

2.1.1 Internal quantum efficiency & Non-radiative recombination center

For the double heterostructure active region, the injected current provides a generation processes as well as carrier leakage provides recombination term. The process of a certain steady-state carrier density in the active region could be compared to that a reservoir analogy, which is being simultaneously filled and drained, as shown in Fig.2.1. In Fig.2.1, there are $\eta_i = (\frac{I}{eV})$ electrons per second per unit volume being injected into the active region. The η_i, is the fraction of terminal current that generates carriers in the active region and V is the volume of active region.

Thus, the rate equation is determined as

$$\frac{dn}{dt} = G_{gen} - R_{re} \quad (2\text{-}1)$$

where Ggen is the rate of injected electrons and Rrec is the rate of recombining electrons per unit volume in the active region. The recombination process is accompanied with spontaneous emission rate Rsp, nonradiative recombination rate Rnr, and carrier leakage rate Rl, as depicted in Fig. 2.1. Carrier leakage rate, R_l, is occurred when the transverse or lateral potential barriers are not sufficiently high. Thus, total recombination rate is expressed as below

$$Rrec = R_{sp} + R_{nr} + R_l \quad (2\text{-}2)$$

It is common to describe the natural decay processes by a carrier lifetime, τ. In the absence of photon generation term, the rate equation for carrier density is,

$$\frac{dn}{dt} = \frac{n}{\tau}, where \frac{n}{\tau} = R_{sp} + R_{nr} + R_l \tag{2-3}$$

The carrier rate equation in the equivalent be expressed as

$$\frac{dn}{dt} = Ggen - Rrec = (\frac{I}{eV}) - \frac{n}{\tau} \tag{2-4}$$

The spontaneous photon generation rate per unit volume is exactly equal to the spontaneous electron recombination rate, Rsp, since by definition every time an electron-hole pair recombines radiatively, a photon is generated. Under steady-state conditions, ($dn/dt = 0$), the generation rate equals the recombination rate,

$$(\frac{I}{eV}) = \frac{n}{\tau} = R_{sp} + R_{nr} + R_l \tag{2-5}$$

The spontaneously generated optical power, Psp, is obtained by multiplying the number of photons generated per unit time per unit volume, Rsp, by the energy per photon, $h\nu$, and the volume of the active region V. Then

$$P_{sp} = h\nu \times V \times R_{sp} = \eta_i \eta_r \frac{h\nu}{e} I \tag{2-6}$$

where the radiative efficiency, η_r, is defined as

$$\eta r = \frac{Rsp}{R_{sp} + R_{nr} + R_l} \tag{2-7}$$

Usually, the η_r depends on the carrier density and the product of $\eta i \eta_r$ is the internal efficiency, η_{int}. Thus according to Eq (2-6), the internal quantum efficiency is defined as:

$$\eta_{\text{int}} = \frac{Psp/(h\nu)}{I/e} = \eta_i \eta_r \tag{2-8}$$

Internal quantum efficiency:

$$IQE = \frac{(the\ \ number\ \ of\ \ photons\ \ emitted\ \ from\ \ active\ \ region\ \ per\ \ second)}{(the\ \ number\ \ of\ \ electrons\ \ injected\ \ into\ \ LED\ \ per\ \ second)} \qquad (2\text{-}9)$$

Thus the internal quantum efficiency is related to η_i, the fraction of terminal current that generates carriers in the active region, and to η_r,the fraction of rates between radiative recombination to total carrier' recombination. According to Eq (2-8), we can enhance the internal quantum efficiency of LEDs by either increasing radiative recombination rate, R_{sp}, or decreasing nonradiative recombination rate, R_{nr}, and carrier leakage rate, R_l.

The possible recombinant paths of injected electrons and holes are shown in Fig. 2.2. Typically, material defect – including defects that extend over some distance of the material such as threading dislocation and more localized point defects such as vacancies and impurities – act as centers of nonradiaive recombination. Thus the overall goal in this stage is to enhance the radiative recombination rate and suppress the nonradiaive recombination rate. Therefore, significantly improvements of grown-layers quality associating with appropriate design of LEDs structure is the main thought to improve the internal quantum efficiency.

2.1.2 The limits of light extraction efficiency

A cross section schematic diagram of typical LED structures is shown in Fig. 2.3(a). The most serious problem with rectangular cubic may be that the photons generated at a point in

the active region will be trapped inside the GaN and sapphire region as shown in Fig. 2.3(b), due to the continued total internal reflections off the chip wall as illustrated in Fig. 2.4. Assume that the angle of incidence in the semiconductor at the semiconductor-air interface is given by θ_1. Then the angle of incidence of the refracted ray, θ_2, can be derived from Snell's law

$$n_s \sin\theta_1 = n_a \sin\theta_2 \tag{2-10}$$

Where, ns and na are the refractive indices of semiconductor and air, respectively. The critical angel θ_c for total internal reflection is obtained using θ_2=90°, using Snell's law, one obtains.

$$\sin\theta_c = \left(\frac{n_a}{n_s}\right)\sin 90°, \theta_c = \sin^{-1}\left(\frac{n_a}{n_s}\right) \tag{2-11}$$

The angle of total internal reflection defines the light-escape cone as shown in Fig. 2.5. Light emitted into the cone can escape from the semiconductor, whereas light emitted outside the cone is suffered from total internal reflection. The surface area of the escape cone is given by the integral

$$Area = \int dA = \int_{\theta=0}^{\theta_c} 2\pi r \sin\theta_r d\theta = 2\pi r^2 (1-\cos\theta_c) \tag{2-12}$$

Assume that light is emitted from a point-like source in the semiconductor with a total power of Psource. Then the power that can escape from the semiconductor is given by

$$P_{escape} = P_{source} \frac{2\pi r^2 (1-\cos\theta_c)}{4\pi r^2} \tag{2-13}$$

Where $4\pi r^2$ is the entire surface area of the sphere with radius r. The calculation indicates that only a refraction of the light emitted inside a semiconductor can escape from the

semiconductor. This fraction is given by

$$\eta_{ext} = \frac{P_{escape}}{P_{source}} = \frac{2\pi r^2(1-\cos\theta_c)}{4\pi r^2} \tag{2-14}$$

Expanding Eq. (2-14) into power series and neglecting higher than second-order term yields

$$\eta_{ext} = \frac{1}{2}\left[1-\left(1-\frac{\theta_c^{\,2}}{2}\right)\right] = \frac{1}{4}\theta_c^{\,2} \approx \frac{1}{4}\frac{n_a}{n_s}, n_a = 1, n_s = n_{GaN} = 2.45 \tag{2-15}$$

According to Eq. (2-15), only a few percent (~4%) of the light generated in the semiconductor can escape from a planar LED.

2.2 Key issues for realizing high efficiency LEDs

2.2.1 Quality issues of GaN epitaxial layers

The GaN-baced material and devices are often epitaxially grown on foreign substrate, such as silicon, silicon carbon (SiC) or sapphire. These substrates must be used because wafers of GaN are very expensive and not easily accessible like other common semiconductors. The nucleation layer, a layer grown at lower temperature, is used to initiate oriented growth on the substrate, followed by epitaxial growth on this layer at higher temperature. The as grown GaN epitaxial layer has high threading dislocation density (TDD) typically in the range of $10^{8\text{-}10}$cm^{-2} due to the mismatched in lattice constants (16%) and thermal expansion coefficients (39%) between GaN and sapphire, resulting in defect-mediated nonradiative recombination of electron-hole pairs and reduced mobility because of carriers trapped by the center of defect. These threading dislocation densities need to be drastically

reduced because dislocations quench light emission of LEDs. These dislocation defects can be reduced by substrate patterning technique such as epitaxial lateral overgrowth (ELOG) [1], or pattern sapphire substrate [2], above approaches depend on spatial filtering, terminating, and turning of threading dislocation, so they do not reach the active region of active region. In this thesis, we report the defect passivation model to effectively block threading dislocation from the substrate to the active region. In particular, defect selective passivation structure not only block the propagation of threading dislocation but also can act as light scattering sites to improve LEDs light extraction efficiency, similar to the use of patterned GaN/sapphire interface to reduce light trapped by total internal reflection.

2.2.2 Light extraction of GaN LEDs

Limitations in light extraction come from total internal reflection at interfaces and light absorption within the device or in the packaging. The generation of light in active region of an LED is most captured with GaN and sapphire by the guided modes. It is due to the high contrast refractive index at the GaN(n=2.45)/air(n=1) and GaN/sapphire(n=1.78) interfaces, resulting in total internal reflection that traps light in the high refractive index and in sapphire substrate. To improve the light extraction efficiency, there are several methods reported, such as patterned sapphire substrates, surface texturing, and air-void formation by nano-patterning.

2.3 Wet etching

2.3.1 Defect properties on GaN surface

Successful fabrication of GaN-based devices depends on the ability to grow epilayer on substrates such as sapphire or silicon carbide, with a low density of defects.[3,4] A high density (10^{8}~10^{10} cm^{-2}) of threading dislocations results from the lattice constant and thermal expansion coefficient mismatch in the nitride film.[5-7] We knew that these defects have influence on both the electrical and optical properties of the material.[8,9] Therefore, the availability of reliable and quick methods to investigate the defects and dislocations in GaN is of great interest.

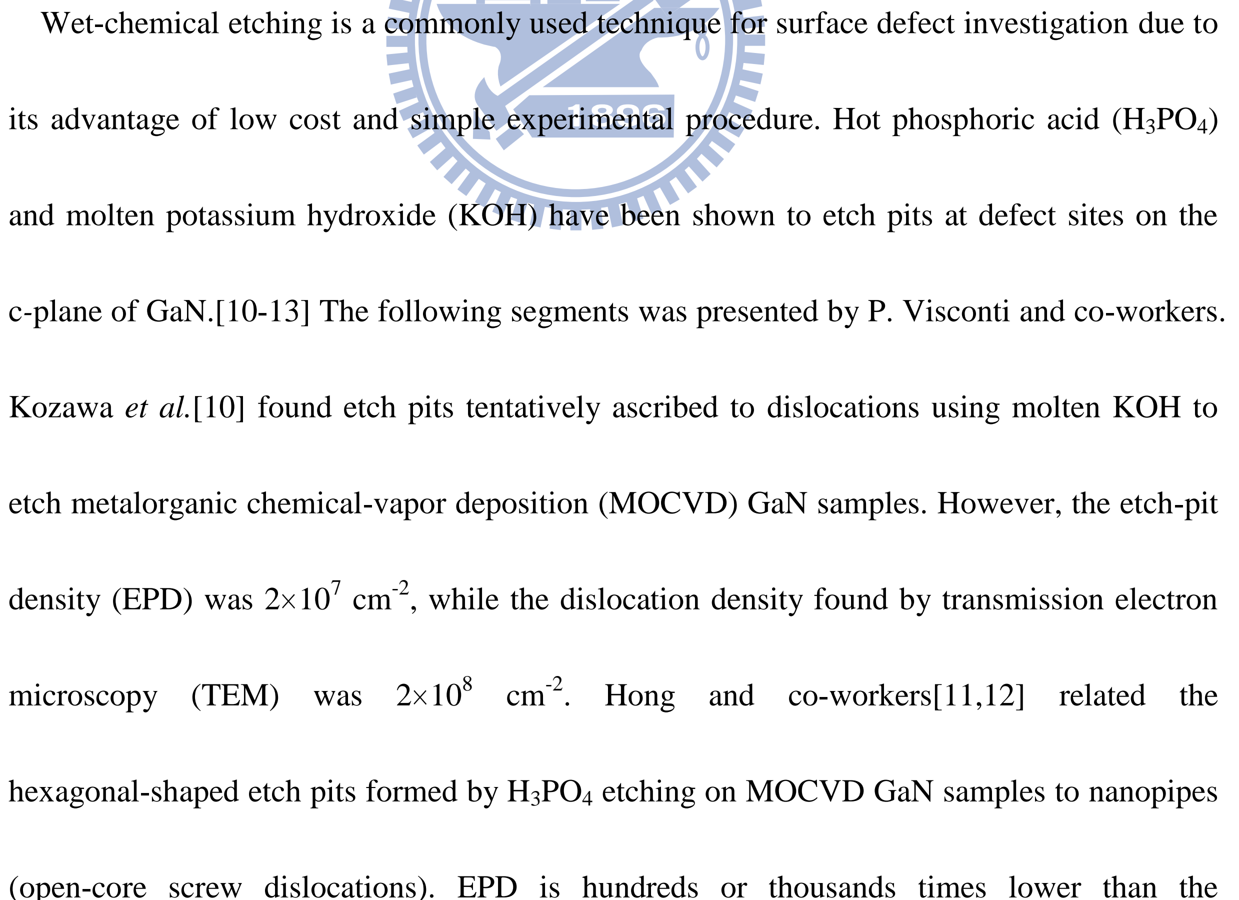

Wet-chemical etching is a commonly used technique for surface defect investigation due to its advantage of low cost and simple experimental procedure. Hot phosphoric acid (H_3PO_4) and molten potassium hydroxide (KOH) have been shown to etch pits at defect sites on the c-plane of GaN.[10-13] The following segments was presented by P. Visconti and co-workers. Kozawa *et al.*[10] found etch pits tentatively ascribed to dislocations using molten KOH to etch metalorganic chemical-vapor deposition (MOCVD) GaN samples. However, the etch-pit density (EPD) was 2×10^{7} cm^{-2}, while the dislocation density found by transmission electron microscopy (TEM) was 2×10^{8} cm^{-2}. Hong and co-workers[11,12] related the hexagonal-shaped etch pits formed by H_3PO_4 etching on MOCVD GaN samples to nanopipes (open-core screw dislocations). EPD is hundreds or thousands times lower than the

dislocation density evaluated by TEM. Lu[13] investigated etch pits formed on MOCVD GaN samples by molten KOH etching. By atomic-force microscopy (AFM) and TEM analyses, they attributed the origin of etch pits. Besides, the origin of etch pits is still controversial and the obtained EPD (in the range $4\times10^{5}\sim1\times10^{8}$ cm^{-2}) is lower than the dislocation density ($10^{8}\sim10^{10}$ cm^{-2}) found by TEM. The etch pits size varies even in the same sample. The shapes of etch pits are well correlated with types of defects, and the etch pits density (EPD) may correspond to the density of defects. However, for GaN, the density, types, and distribution of defects vary significantly due to growth-related conditions, which makes it difficult to reach an agreement about the origin of the etch pits, and it can be even more difficult for test techniques.

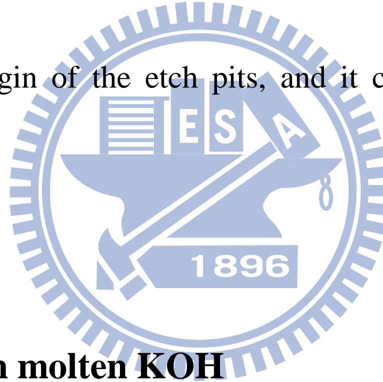

2.3.2 Etching process in molten KOH

The discrepancy of etching characteristics in Ga-face (+c GaN, Ga-polarity) and N-face (-c GaN, N-polarity) has been specifically investigated as illustrated in Fig. 2.6. Some reports showed that gallium nitride could be etched in the aqueous sodium hydroxide (NaOH) solution but etching ceased when the formation of an insoluble coating of presumably gallium hydroxide ($Ga(OH)_3$) [14,15]. For further etching, it would need removing of the coating by continual jet action. Various aqueous acid and base solutions have been tested for etching of GaN were list in Table 2.1 [16-18]. The undetermined etch rate (nm/min) was because it

various from sample to sample and differences in the defect density. According to the research reports in recent years; the common cognition related to gallium nitride etching process was that the most of gallium nitride could be etched rapidly in N-face. The reason for the face-dependent gallium nitride etching process has been studied by Li *et al.*, who utilized the X-ray photoelectron spectroscopy (XPS) to examine the surface chemistries before and after etching process in aqueous KOH solutions for both Ga- and N-face gallium nitride. The conclusion is that the different etching results in Ga- and N-face gallium nitride crystals are due to the different states of surface bonding. Besides, the most important is the etching process only dependent on the polarities, not on the surface morphology, growth condition and which atoms form the surface termination layer. The GaN chemical etching reaction with KOH could be described as the following formula [19]:

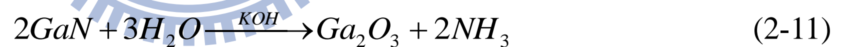

$$2GaN + 3H_2O \xrightarrow{KOH} Ga_2O_3 + 2NH_3 \quad (2\text{-}11)$$

Here, the molten KOH act as a catalyst and a solvent for the resulting Ga2O3 (Fig. 2.7 (d)) as well. The mechanism about etching N-face gallium nitride substrate was illustrated in Fig. 2.7. The hydroxide ions (OH^-) were first absorbed on the gallium nitride surface (Fig. 2.7 (b)) and finally react with Ga atoms once the OH^- ions with sufficient kinetic energy as shown in the Fig. 2.7 (c). The etching could be started at step (c) if the surface was Ga-terminated. The inertness of Ga-face GaN was ascribed to the hydroxide ions would be repelled by the negatively-charged triple dangling bonds of nitrogen near the surface. Thus, if the Ga-face

GaN was Ga-terminated, the etching process stops after the first gallium atom layer was removed. In contrast, for the N-face GaN, every nitrogen atom bears a single dangling bond to prevent the hydroxide ions attacking from Ga atoms.

Table. 2.1 Various chemicals etch GaN.[20]

Chemical	Temperature (°C)	Etch rate (μm/min)	Etching planes observed
Acetic acid (CH_3COOH)	30	<0.001	None
Hydrochloric acid (HCl)	50	<0.001	None
Nitric acid (HNO_3)	81	<0.001	None
Phosphoric acid (H_3PO_4)	108–195	0.013–3.2	$\{10\bar{1}\bar{2}\},\{10\bar{1}3\}$
Sulphuric acid (H_2SO_4)	93	<0.001	None
Potassium hydroxide (KOH), molten	150–247	0.003–2.3	$\{10\bar{1}0\},\{10\bar{1}\bar{1}\}$
50% KOH in H_2O	83	<0.001	None
10%–50% KOH in ethylene glycol (CH_2OHCH_2OH)	90–182	0.0015–1.3	$\{10\bar{1}0\}$
50% NaOH in H_2O	100	<0.001	None
20% NaOH in ethylene glycol	178	0.67–1.0	None

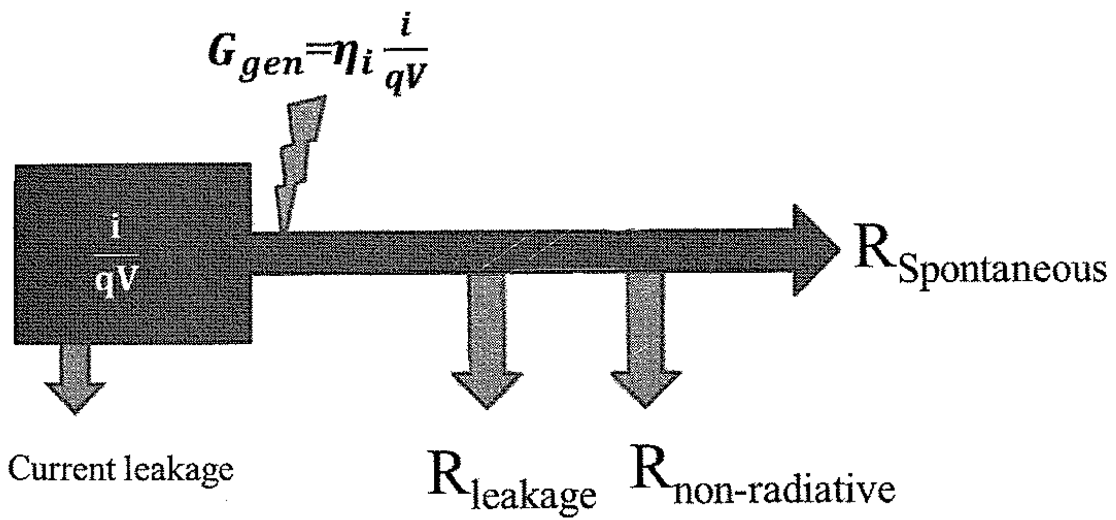

Fig. 2.1 Schematic analogy carriers injected into active regions and depletion through radiative, onradiative, and leakage recombinations. [21]

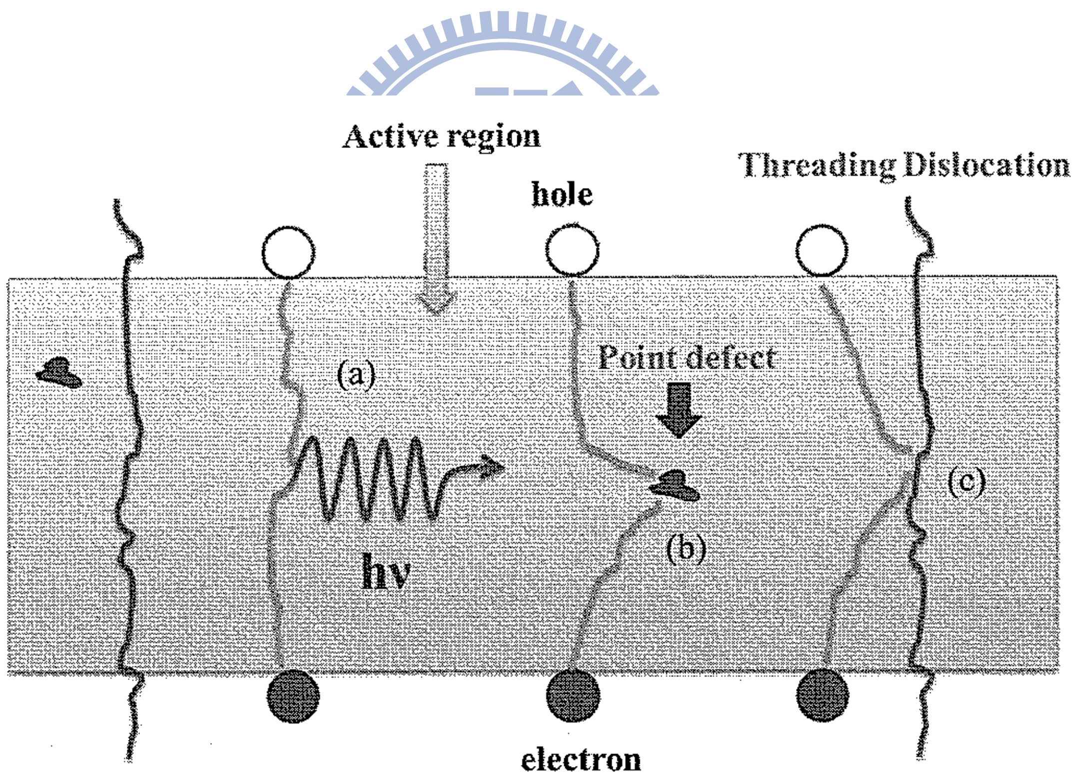

(a) Radiative path

(b) and (c) Non-radiative path

Fig. 2.2 Radiative and non-radiative recombination in active region. [21]

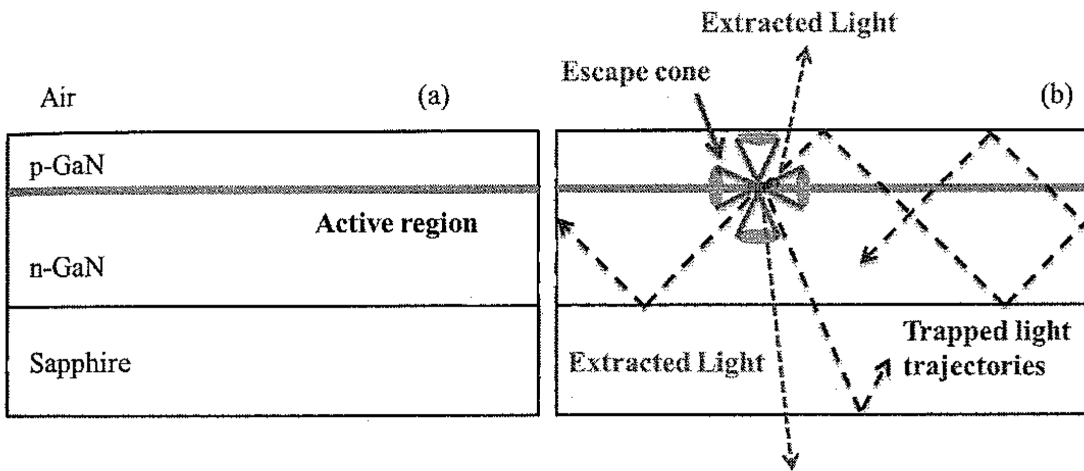

Fig. 2.3 (a) Cross section schematic diagram of typical LED structures (b) Photon trajectories inside the LED. [21]

Fig. 2.4 Total internal reflection in GaN-based LED. [21]

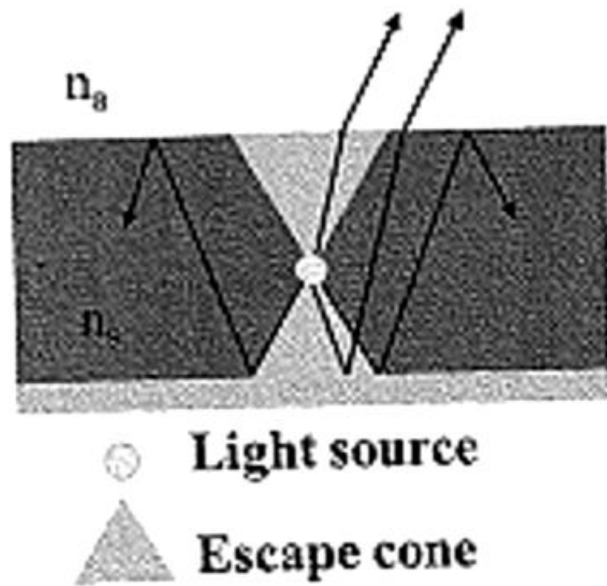

Fig. 2.5 The angle of total internal reflection defines the light-escape cone. [21]

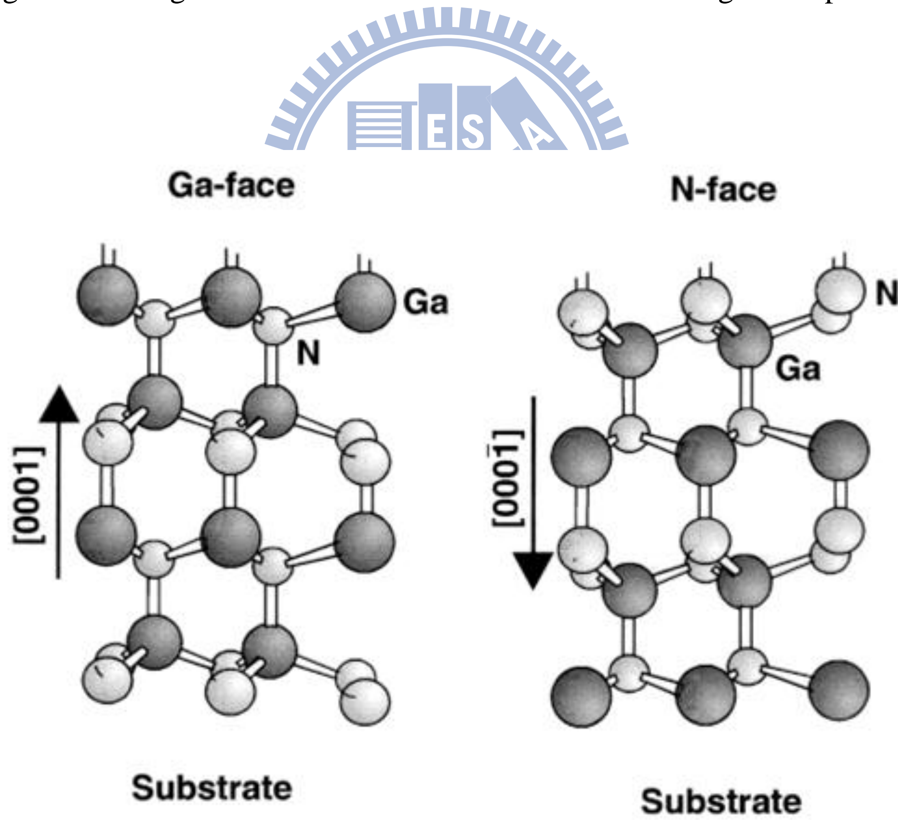

Fig. 2.6 Illustration of different polarity, (a) Ga-face (+c GaN, GaN polarity), (b) N-face (-c GaN, N-polarity). [22]

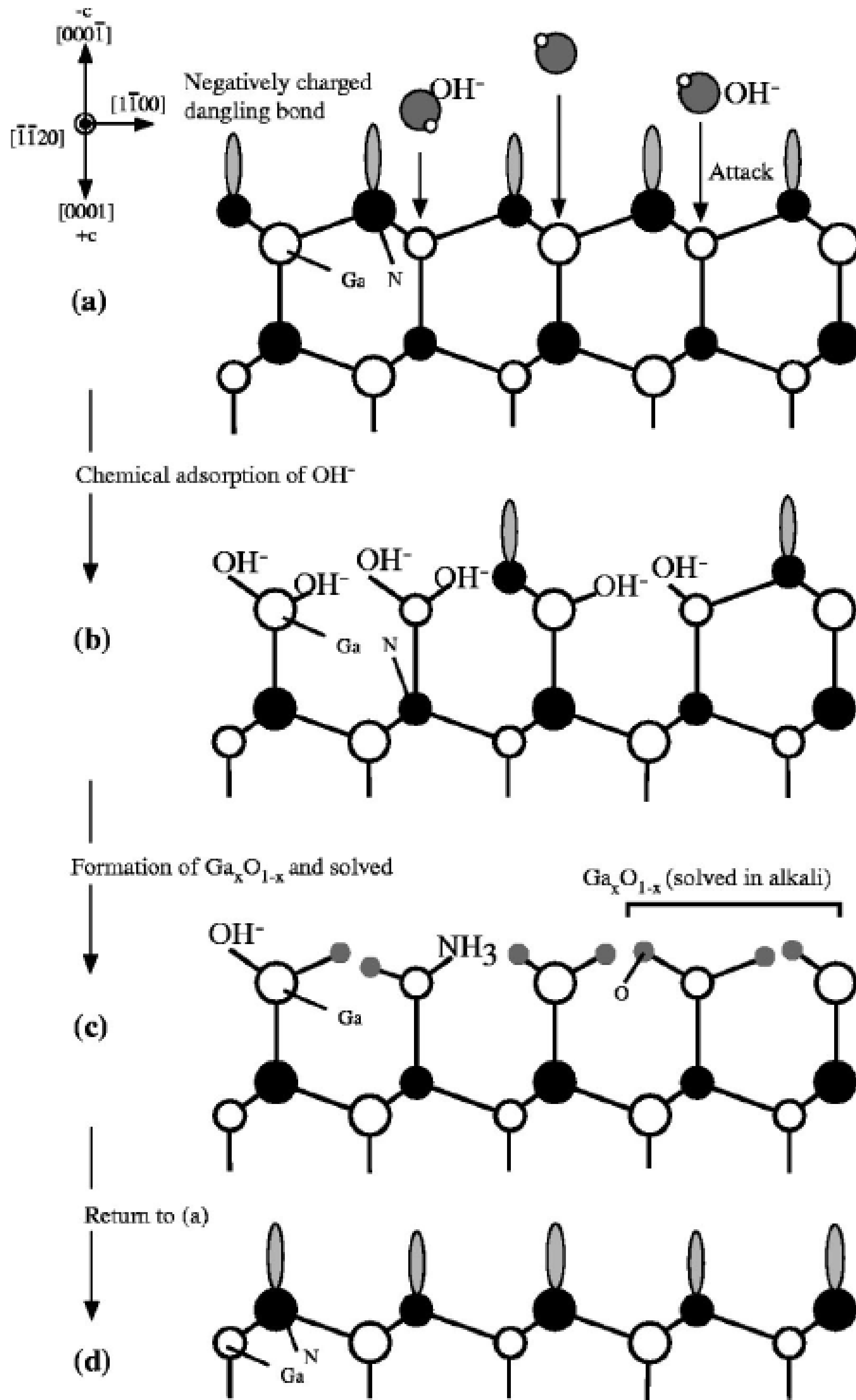

Fig. 2.7 Schematic diagrams of the cross section GaN film viewed along [-1-120] direction for N-polar GaN to explain the mechanism of the polarity selective etching. (a) Nitrogen terminated layer with one negatively charged dangling bond on each nitrogen atom; (b) absorption of hydroxide ions; formation of oxides; (d) dissolving the oxides. [23]

2.4 Reference

[1] A. Usui, H. Sunakawa, A. Sakai and A. A. Yamaguchi, Jpn. *J. Appl. Phys*. **36**, L889 (1997).

[2] M. Yamada, T. Mitani, Y, Narukawa, S. Shioji, I. Niki, S. Sonobe, K. Deguchi, M. Sano and T. Mukai, Jpn. *J. Appl. Phys.* **41**, L1431 (2002).

[3] H. Morkoc¸, S. Strite, G. B. Gao, M. E. Lin, B. Sverdlov, and M. Burns, *J. Appl. Phys.* **76**, 1363 (1994).

[4] S. Nakamura, T. Mukai, and M. Senoh, *Appl. Phys. Lett.*, **64**, 1687 (1994).

[5] S. D. Lester, F. A. Ponce, M. G. Craford, and D. A. Steigerwald, *Appl. Phys. Lett.* **66**, 1249 (1995).

[6] W. Qian, M. Skowronski, M. DeGraef, K. Doverspike, L. B. Rowland, and D. K. Gaskill, *Appl. Phys. Lett.* **66**, 1252 (1995).

[7] X. H. Wu, L. M. Brown, D. Kapolnek, S. Keller, B. Keller, S. P. Den-Baars, and J. S. Speck, *J. Appl. Phys.* **80**, 3228 (1996).

[8] B. Garni, J. Ma, N. Perkins, J. Liu, T. F. Kuech, and M. G. Lagally, *Appl. Phys. Lett.* **68**, 1380 (1996).

[9] S. J. Rosner, E. C. Carr, M. J. Ludowise, G. Girolami, and H. I. Erikson, *Appl. Phys. Lett.* **70**, 420 (1997).

[10] T. Kozawa, T. Kachi, T. Ohwaki, Y. Taga, N. Koide, and M. Koike, J. Electrochem. Soc. **143**, L17 (1996).

[11] S. K. Hong, T. Yao, B. J. Kim, S. Y. Yoon, and T. I. Kim, Appl. Phys. Lett. **77**, 82 (2000).

[12] S. K. Hong, B. J. Kim, H. S. Park, Y. Park, S. Y. Yoon, and T. I. Kim, J.Cryst. Growth **191**, 275 (1998).

[13] L. Lu, Z. Y. Gao, B. Shen, F. J. Xu, S. Huang, Z. L. Miao, Y. Hao, Z. J. Yang, G. Y. Zhang, X. P. Zhang, J. Xu, D. P. Yu, *J. Appl. Phys.*, **104**, 123525 (2008)

[14] T.L. Chu, J. Electrochem. Soc. 118, 1200 (1971).

[15] J.I. Pankove, J. Electrochem. Soc. 119, 1118 (1972).

[16] H. Cho, D.C. Hays, C.B. Vartuli, S.J. Pearton, C.R. Abernathy, J.D. MacKenzie, F. Ren, J.C. Zolper, Mater. Res. Soc. Symp. Proc. 483, 265 (1998).

[17] C.B. Vartuli, S.J. Pearton, C.R. Abernathy, J.D. MacKenzie, F. Ren, J.C. Zolper, R.J. Shul, *Solid-State Electron*. 41 (12), 1947 (1998).

[18] S.J. Pearton, R.J. Shul, Gallium nitride I, in: J. Pankove, T.D. Moustakas (Eds.), Semiconductor and Semimetals Series, vol. 50, Academic Press, New York, NY, p. **103** (1998).

[19] D. Li, M. Sumiya, S. Fuke, D. Yang, D. Que, Y. Suzuki, Y. Fukuda, *J. Appl. Phys.* **90**, 4219 (2001).

[20] D. A. Stocker, E. F. Schubert and J. M. Redwing, Appl. Phys. Lett., Vol. 73, No. 18, 2 November (1998).

[21] Growth and fabrication of high efficiency GaN based light emitting devices. M. H. Lo

[22] O Ambacher, J. Phys. D: Appl. Phys. 31 2653–2710 (1998)

[23] Dongsheng Li, M. Sumiya, S. Fuke, Deren Yang, Duanlin Que, Y. Suzuki and Y. Fukuda, J. Appl. Phys., Vol. 90, No. 8, 15 October 2001

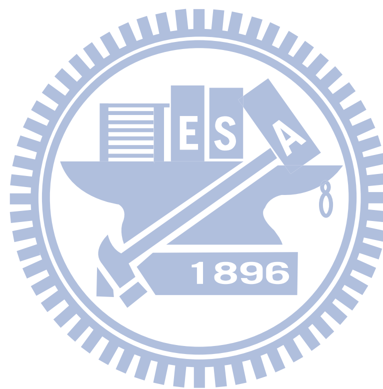

Chapter 3

3.1 Scanning electron microscopy (SEM)

The scanning electron microscope is built of the following parts:

(i) The electron gun

(ii) The system of three-stage electromagnetic lens is used to demagnify (focus, condense) the electron beam diameter to 5~10 nm at the specimen.

(iii) Detectors may detect electrons, X-ray or cathodo-luminescent (CL) light.

(iv) The microscope column is evacuated to 10^{-5} torr.

Fig. 3.1 shows that schematic diagram of a scanning electron microscope (SEM). Two pairs of deflection coils are shown in the SEM column. This double deflection allows the scanning beam to pass through the final aperture. Four pairs are actually used, for double deflection in *x* and *y* directions.

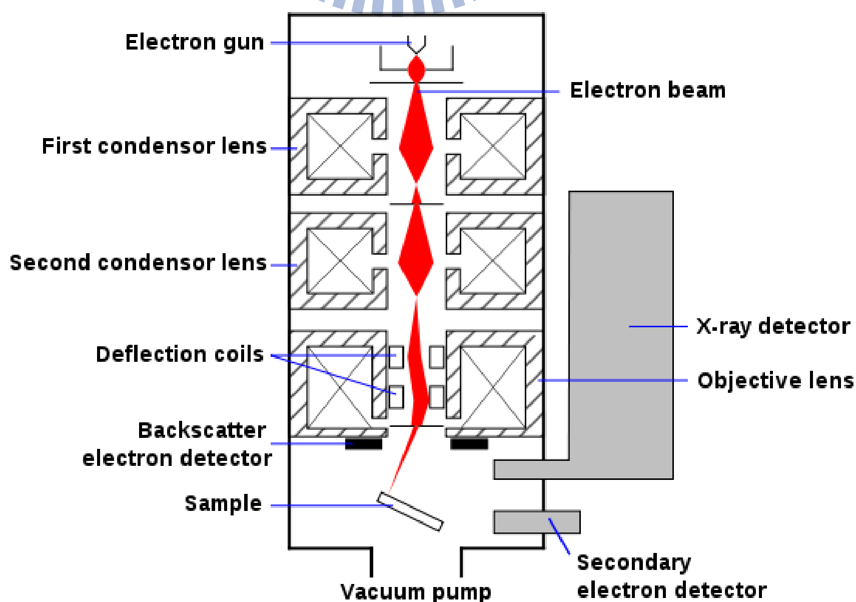

Fig. 3.1 Schematic diagram of a scanning electron microscope (SEM).[1]

SEM is a technique which forms an image of microscopic region of the specimen surface. An electron beam from 5~10 nm in diameter is scanned across the specimen. The interaction of the electron beam with the specimen produces a series of phenomena such as:

(i) backscattering of electrons of high energy

(ii) secondary electrons of low energy

(iii) absorption of electrons

(iv) X - ray

(v) visible light (cathodoluminescence, CL)

Fig. 3.2 indicates that any of these signals can be continuously monitored by detectors.

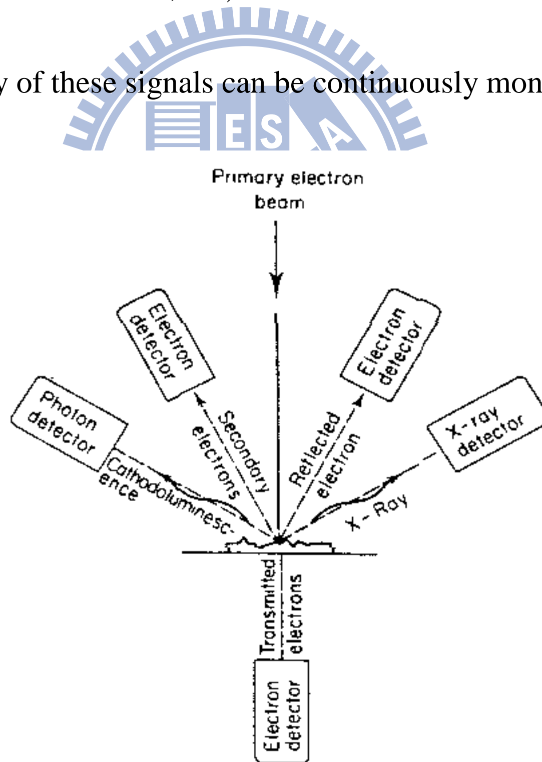

Fig. 3.2 Information that can be generated in the SEM by an electron beam striking the sample.[2]

3.2 Cathodoluminescent spectroscopy (CL)

Cathodoluminescence (CL) is a SEM-based technique that can be used for analyzing the characteristic of semiconductor materials and devices. CL is the emission of light as the result of electron or “cathode-ray” bombardment. SEM-based and CL can provide information on the concentration and distribution of luminescent centers, distribution and density of electrically active defects, and electrical properties including minority carrier diffusion lengths and lifetimes.

Fig. 3.3 JSM-7000F SEM and CL System.

3.3 Atomic Force Microscopy (AFM)

Atomic force microscopy (AFM) or scanning force microscopy (SFM) is a very high-resolution type of scanning probe microscopy (SPM) instead of optical imaging one. In 1986, the AFM was invented by Gerd Binnig, Christoph Gerber, and Calvin F. Quate. The AFM is one of the foremost tools for imaging, measuring, and manipulating matter at the nanoscale. A very tiny, pyramidal probe is attached on the cantilever. The tip must be very tiny (single atom size) with sharp angle for large-area scan.

The AFM utilizes a sharp probe moving over the surface of a sample in a raster scan. When the probe is approaching sample surface, attractive (van der Waals force) or repulsive force (Coulomb repulsion) between tip and sample is formed and detected. Forces between the tip and the sample lead to a deflection of the cantilever according to Hooke's law. The interaction force causes cantilever to shift along z-axis and thus the topology of sample is obtained. The small probe-sample separation (on the order of the instrument's resolution) makes it possible to take measurements over a small area. To acquire an image the microscope-scans the probe over the sample while measuring the local property in question. The resulting image resembles an image on a screen in that both consist of many rows or lines of information placed on above the other. Unlike the traditional microscopes, scanned probe system do not use lenses, so the size of the probe rather than diffraction effect generally limits their resolution.

Followings are the operating mode of AFM, shown as the Figs. 3.4[(a)-(c)]:

1. Contact mode: The Interaction mainly comes from repulsive force between tip and sample. It is easy to obtain atomic-scale resolution, but easy to damage surface of sample.
2. Non-contact mode: The Interaction mainly comes from van der Waals force between tip and sample. The tip never touches sample surface; resolution is lower (~50 nm). The surface of samples is preserved.
3. Tapping mode: The tip touches the surface of samples periodically. The resolution could be as high as contact-mode. The surface of samples could be damaged sometimes.

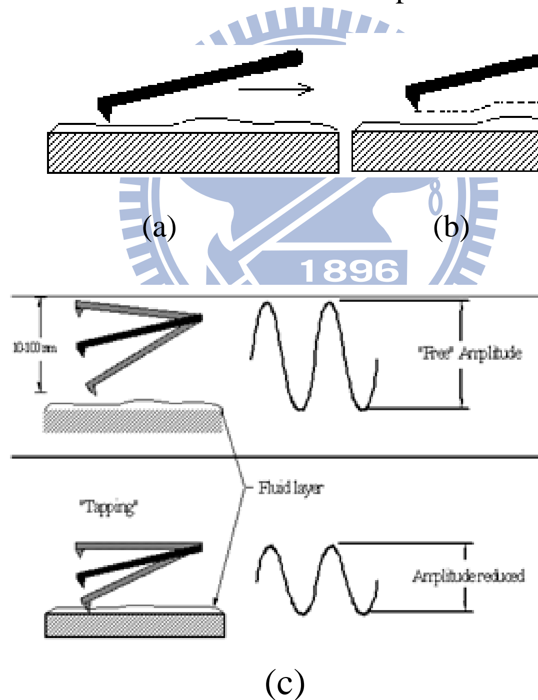

Figures. 3.4[(a)-(c)] Operating mode of AFM (a) contact mode, (b) non-contact mode, (c) tapping mode.[2]

3.4 Micro photoluminescence spectroscopy (μ-PL)

Photoluminescence (PL) spectroscopy has been used as a measurement method to detect the optical properties of the materials because of its nondestructive characteristics. PL is the emission of light from the material under optical excitation. Reducing the laser beam spot size to micrometer by beam expanders and objective lens is the so-called μ-PL. Fig 3.5 illustrates the photoluminescence process. The laser light source used to excite carriers should have large energy band gap than the semiconductors. When the laser light absorbed within the semiconductors, it should excite the carriers from the valence band to the conduction band. Then, is produces the electrons in the conduction band and the holes in the valance band. When the electron in an excited state returns to the initial state, it will emit a photon whose energy is equal to energy difference between the excited state return and the initial state, therefore, we can observe the emission wavelength peak from PL spectrum.

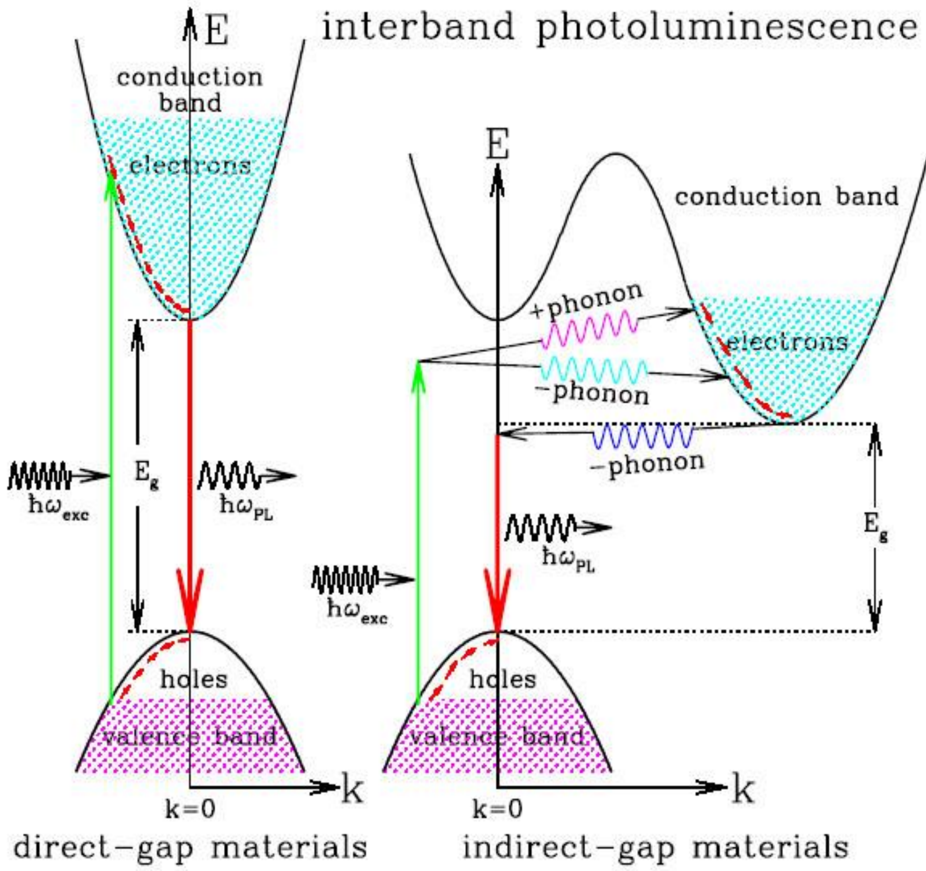

Fig. 3.5 Interband transitions in photoluminescence system.[3]

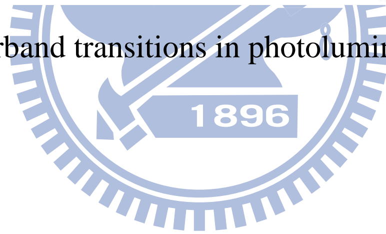

3.5 Electroluminescence spectroscopy (EL)

Electroluminescence (EL) is an optical and electrical phenomenon in which a material emits light in response to an electric current passed through it, or to a strong electric field across the material. This is different from light emission resulted from chemical reaction (chemiluminescence), or other mechanical action (mechanoluminescence).

Electroluminescence is the result of radiative recombination of electrons and holes in the material such as semiconductor. The excited electrons release their energy as photons – light. Prior to recombination electrons and holes are separated either as a result of doping of the material to form a p-n junction such as LED, or through excitation by impact of high energy electrons accelerated by a strong electric field (as with the phosphors in electroluminescent displays).

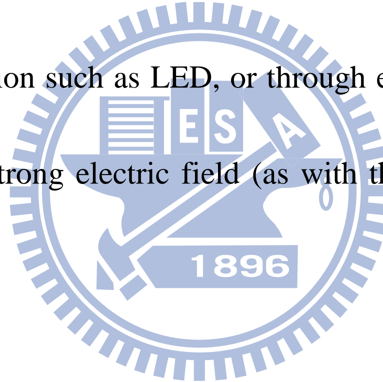

3.6 Reference

[1] http://en.wikipedia.org/wiki/File:Schema_MEB_(en).svg

[2] Class of Materials analysis, S. H. Yang, NCTU in Tainan

[3] http://ned.ipac.caltech.edu/level5/Sept03/Li/Li4.html

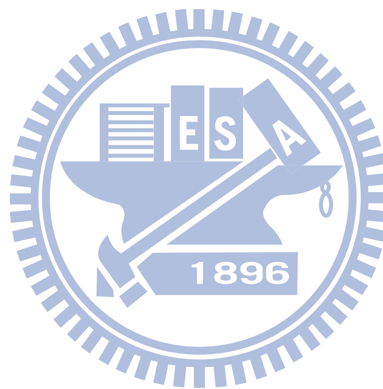

Chapter 4 Result and discussion

4.1 Fabricate LED on the GaN epilayer of defect selective passivation

Figs. 4.1[(a)-(d)] shows the previous process flow of defect selective passivation. In Fig. 4.1(a), the molten KOH or hot H_3PO_4 selectively etch defect sites and form hexagonal pits on GaN surface. To block the propagation of threading dislocation, a 500nm SiO_2 film was deposited on the GaN in Fig. 4.1(b) Then, the SiO_2 thin film on the flat surface is removed by chemical mechanical polishing (CMP). Meanwhile, the SiO_2 in the defect pits still remain untouched as shown in Fig. 4.1(c). The exposed GaN flat surface provides the seed layer for epitaxial regrowth, which grows in both vertical and lateral direction to cover over the SiO_2 passivated pits as shown in Fig. 4.1(d).

The previous process of DSP method is complex and expensive equipment. In this thesis, we do something different from previous process. Figs. 4.2[(a)-(c)] show the schematic of the simplified process. First, the GaN wafers with native pits (NPs) are chosen shown as Fig. 4.2(a). Then we use the SiO_2 nanospheres as mask to block defect pits in GaN epitaxial growth. The process of defect selective blocking by self-assembled silica nanospheres performed through the spin coating method without expensive setup.

The LED structure with 2μm Si-doped n-GaN, 12pairs of InGaN/GaN multi-quantum wells(MQWs), and 30nm Mg doped p-GaN were grown on the template. The QW emission wavelength is at 440nm. A LED without DSP process, a LED coated 40nm silica nanospheres

on GaN defect pits, and a LED coated 100nm silica nanospheres on GaN pits denoted as sample A, B, C, respectively.

4.2 Analysis of defect selective passivation process

Wet chemical etching is commonly used for estimating defects density and defect types. In order to reveal the etched pits from dislocation in GaN and look for any consistency among the various chemical etches, we have used hot H_3PO_4 and molten KOH as defect etchants in GaN, which produce hexagonal-shaped etch pits. By varying the time and temperature, the etching process produces a pitted surface that clearly reveals the size and density of the pits that we need to know. Fig. 4.3 shows that the properties of etch pits depend upon the solution temperature and etched time. When immersing specimen in solution at long time and high temperature, there are often several pits clustered together. Moreover, chemicals overetch the GaN plate.

Surface morphology of samples was characterized by scanning electron microscopy (SEM) and atomic force microscopy (AFM). The SEM image of the GaN sample etched by H_3PO_4 for 2 min at 240 ℃ is shown in Fig. 4.4[(a),(b)]. The etch pits, with a density of about 9.58×10^5 cm^{-2}, are of hexagonal shape and their size ranges from 1.50 to 1.88μm in diameter. Etch pits might be related with threading screw dislocations or nanopipes (open core dislocations)[1,2].

Figure 4.5[(a),(b)] shows that the surface morphology of the GaN sample grown by the same run immersed in molten KOH for 2min30sec at 300°C. The size of the etch pits is about 1μm, and the density of etched pits is 10^6 cm^{-2}. The EPD of the sample etched by KOH is ten times higher than that found for the H_3PO_4-etched sample. Three different shapes of the etch pits were identified with three types of defects originated from screw-, edge-, and mixed-type TDs, respectively. It has been realized that dislocation etch pits etched by molten KOH to identify the origin and mechanism of etch pits in GaN layer[3].

Fig. 4.6(a) indicates that the the defect pits density of GaN with native pits is approximately 10^5~10^6 cm^{-2}. Then the Fig. 4.3(b) shows that a pit is filled with nanospheres.

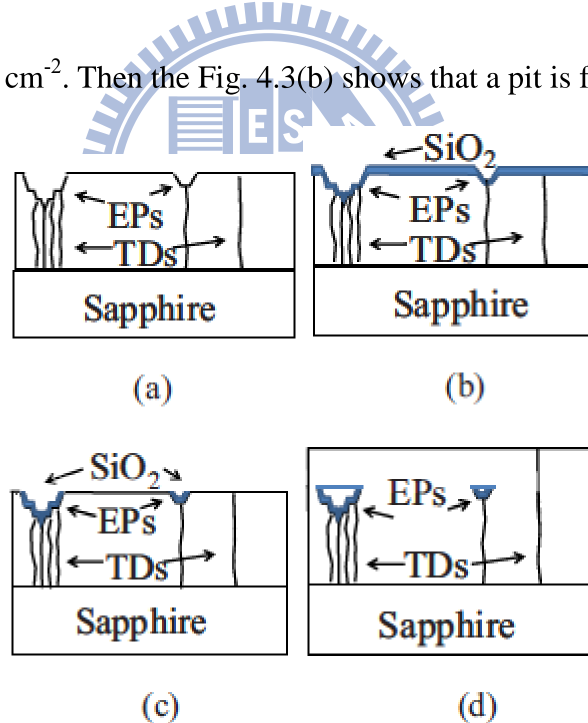

Figs. 4.1[(a)-(d)] Schematic diagrams of defect selective passivation process.

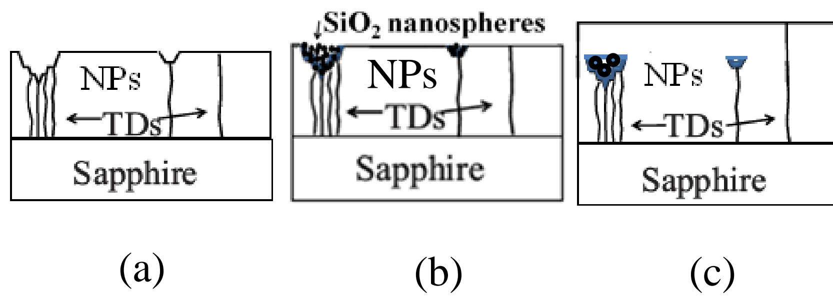

Figs. 4.2[(a)-(c)] Schematic diagrams of simplified defect selective passivation process

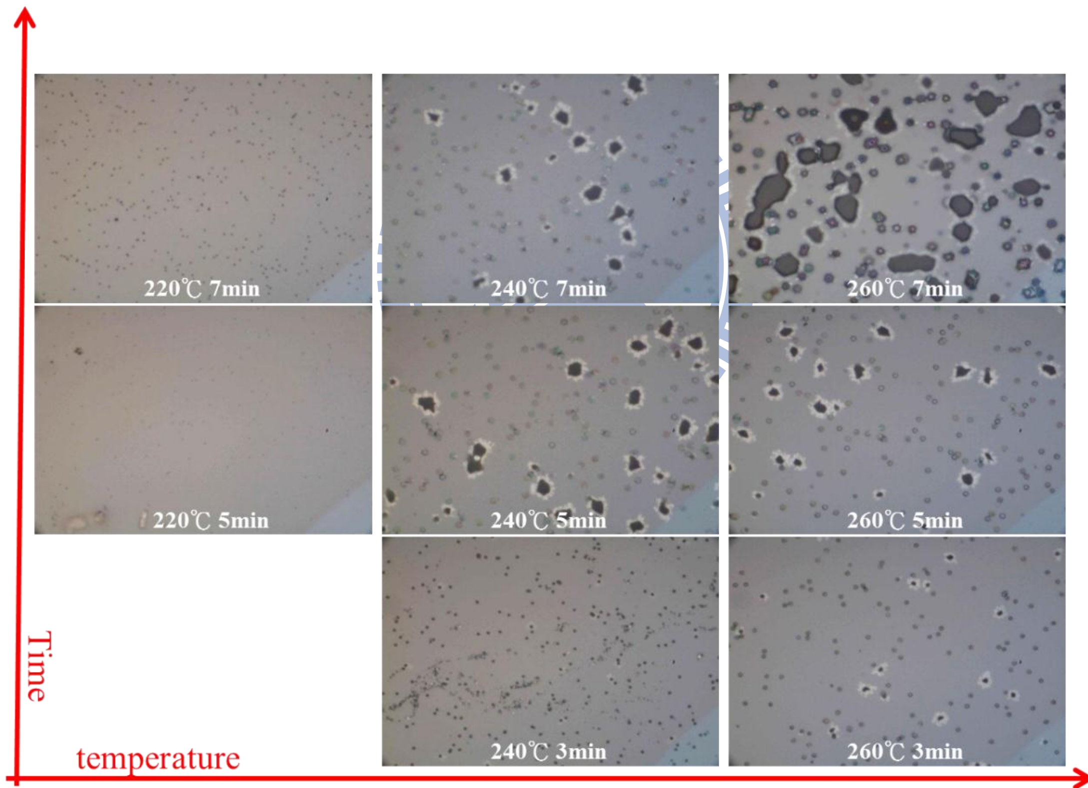

Fig. 4.3 Optical microscopy image of GaN surface etched at varied time and temperature.

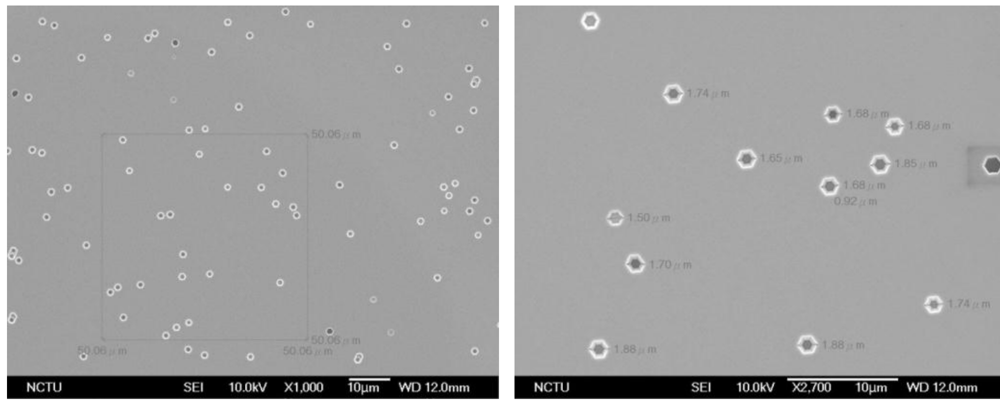

Fig. 4.4 SEM image of GaN surface etched by H_3PO_4. Low (a) and high (b) magnification images.

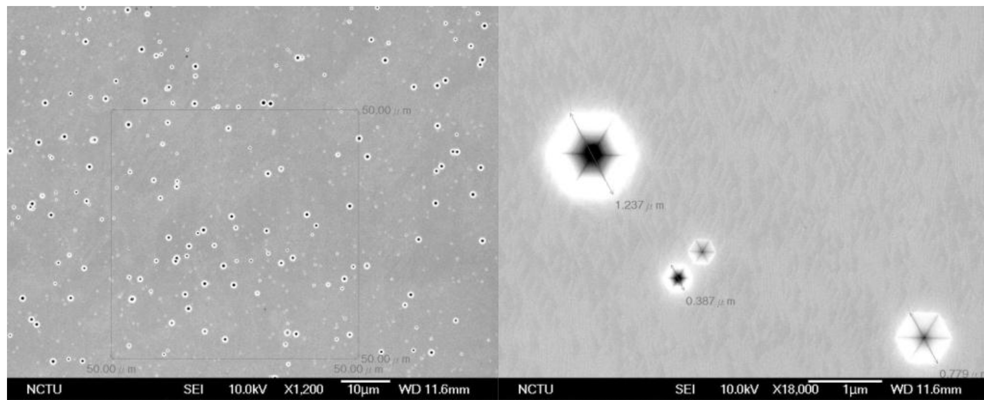

Fig. 4.5 SEM image of GaN surface etched by molten KOH. Low (a) and high (b) magnification images.

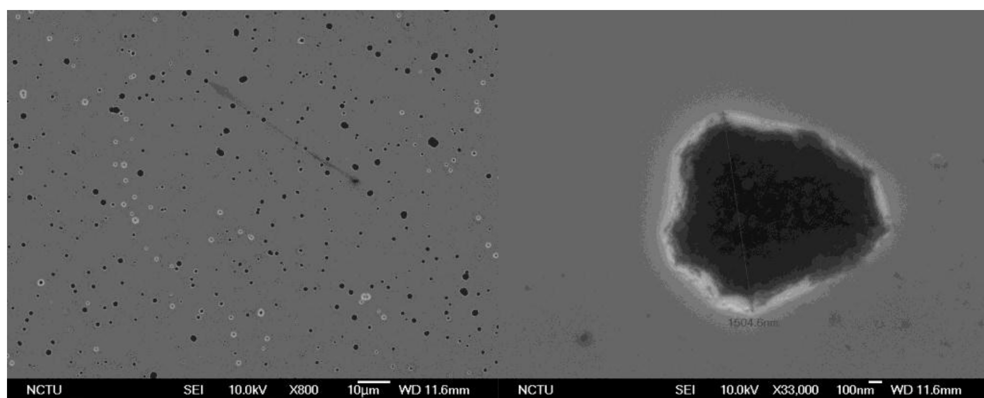

Figs. 4.6[(a),(b)] SEM image of GaN surface spin-coated nanospheres. Low (a) and high (b) magnification images.

4.3 Analysis of DSP-LED performance

4.3.1 Optical properties analysis of LED grown on DSP epilayer

Photoluminescence(PL)

A LED without DSP process, a LED coated 40nm silica nanospheres on GaN defect pits, and a LED coated 100nm silica nanospheres on GaN pits denoted as sample A, B, C, respectively. The LED structure with 2μm n-GaN, 12pairs of InGaN/GaN multi-quantum wells(MQWs), and 30nm p-GaN were grown on the template. The room temperature photoluminescence spectra at 10mW pumping power are shown as Fig. 4.7. The MQWs emission wavelength ranges about at 440nm. The intensity of sample B and C are two or three times than that of sample A. From the result, we think that the crystal quality of GaN epilayer grown with DSP process has been effectively improved.

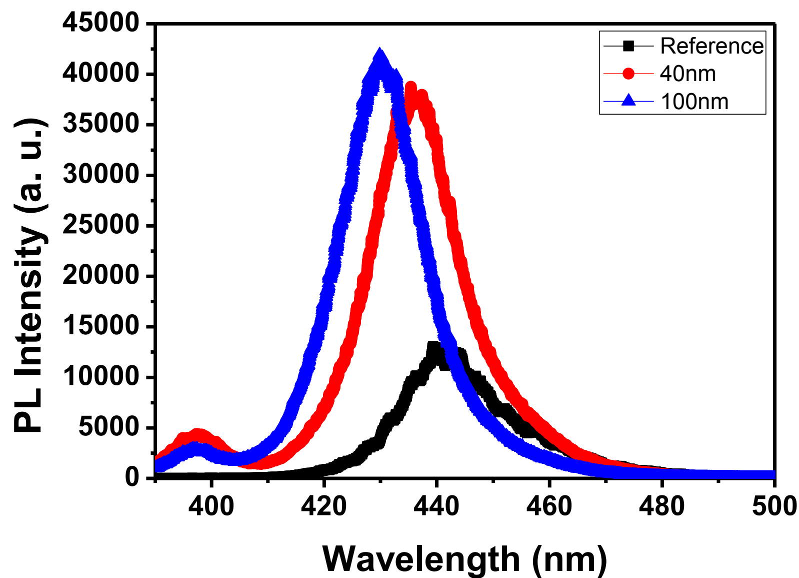

Fig. 4.7 Photoluminescence spectrum

Cathodoluminescent (CL)

The optical characteristic is investigated by SEM cross section and cathodoluminescent images as shown in Figs. 4.8[(a)-(f)]. These images are taken by simply switching detection mode from scattering electron detection to cathodoluminescent detection under the same magnification condition and thus have one to one location correspondence. Comparing to the cross section CL image of different samples, A, B and C, respectively, the DSP methed minimizes the propagation of threading dislocations.

CL plane-view images as observed in Figs. 4.9[(a)-(c)]. The dark spots are corresponding with dislocations. We estimate the density of dark points on different samples, 8.24×10^{7} cm^{-2} at sample A, 5.24×10^{6} cm^{-2} at sample B and 2.94×10^{6} cm^{-2} at sample C. It clearly reveals that the nanospheres effectively block the propagation of threading dislocations but also reduce the density of defect pits. The threading dislocation defects are the strong non-radiative recombination centers[4]. The significant increase in CL intensity demonstrates that the loss of excited carriers due to non-radiative recombination is greatly reduced in the defect passivated layer as a result of reduction in TD density.

4.3.2 Electrical properties analysis of LED grown on DSP epilayer

LED chips with size of 300×300 μm^2 were fabricated from the defect selective passivation epi-wafer. The electrical characteristics are compared with a reference-LED going through the

same fabrication process except for the defect passivation structure. The light-current (L-I) and voltage-current (V-I) curves of LEDs are shown in Fig. 4.11. Furthermore, the optical power was collected by an integrating sphere to make sure that radiation in all directions was collected. The L-I curve in Fig. 4.11 indicates that the optical output power of DSP-LEDs are much higher than that of reference-LED. The silica masks not only block the propagation of threading dislocation but also act as light scattering sites which reduce light trapped by total internal refection (TIR) to enhance light extraction efficiency. Between the reference-LED and DSP-LED passivated by 40nm SiO_2 nanospheres, the output power of DSP LED exhibits 46%, 39%, 25% and 18% enhancement at 50mA, 100mA, 150mA and 200mA, respectively. Meanwhile, the output power exhibits 45%, 38%, 25% and 17% enhancement at respectively 50mA, 100mA, 150mA and 200mA, when comparing reference-LED and DSP-LED passivated by 100nm SiO_2 nanospheres.

Fig. 4.12 shows the reverse voltage versus current characteristics of DSP-LEDs and ref-LED. The leakages come from the non-radiative recombination of screw type dislocations. As observed in Fig. 4.12, we believe that the defect passivation process does not introduce more screw defects[5]. As the above mentioned, the defect selective passivation method can reduce threading dislocations and improve GaN epilayer quality.

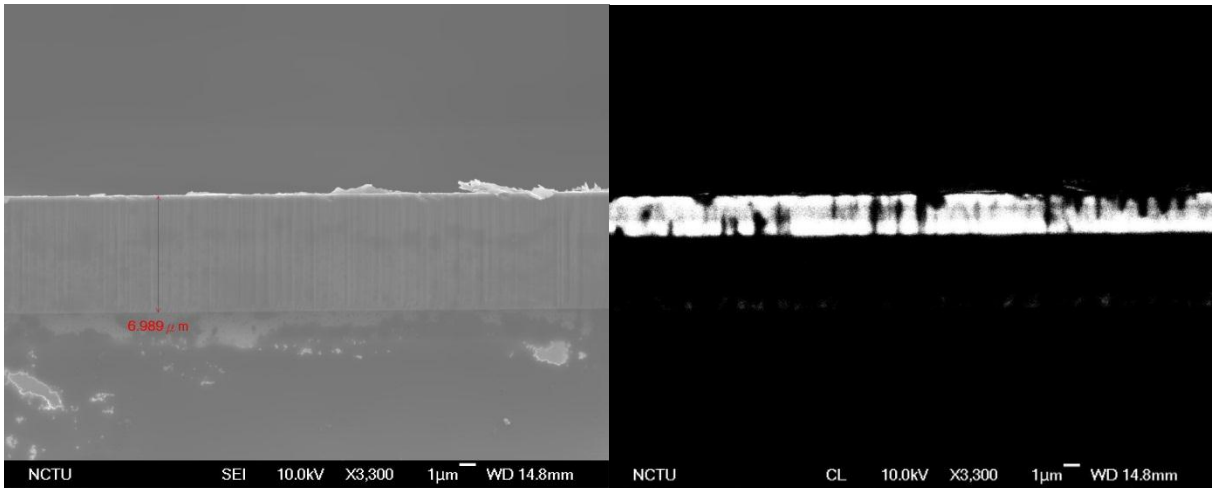

Sample A (a) (d)

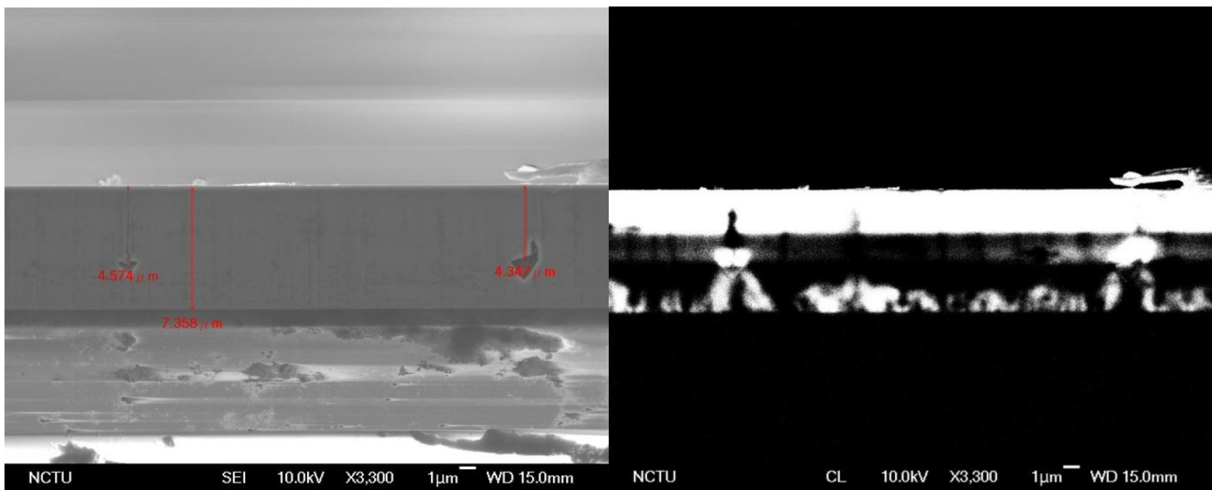

Sample B (b) (e)

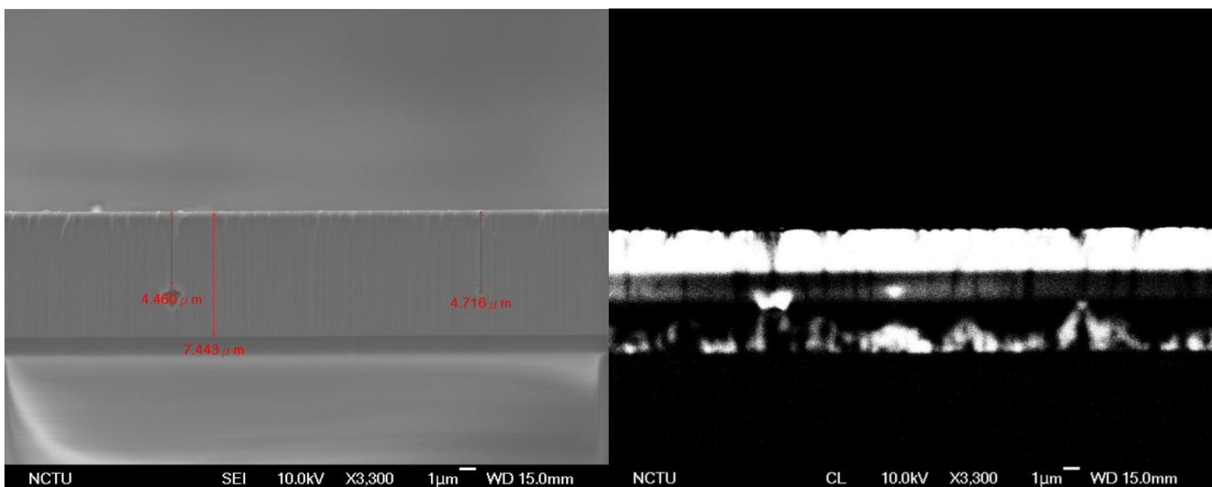

Sample C (c) (f)

Figs. 4.8[(a)-(f)] [(a)-(c)] SEM and [(d)-(f)] CL cross section image of the defect selective passivatied epi-wafer under the same magnification.

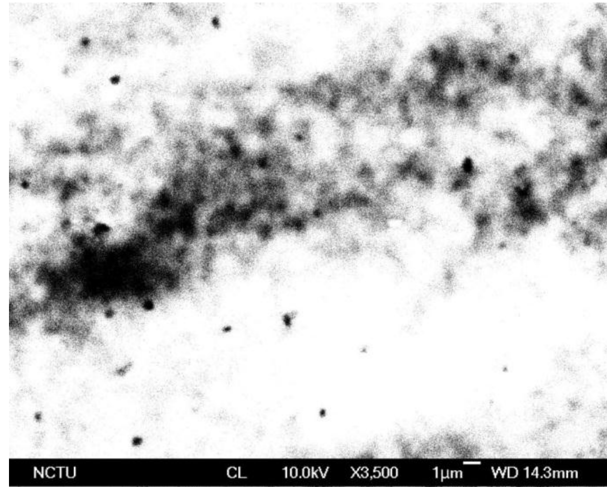

(a) Sample A

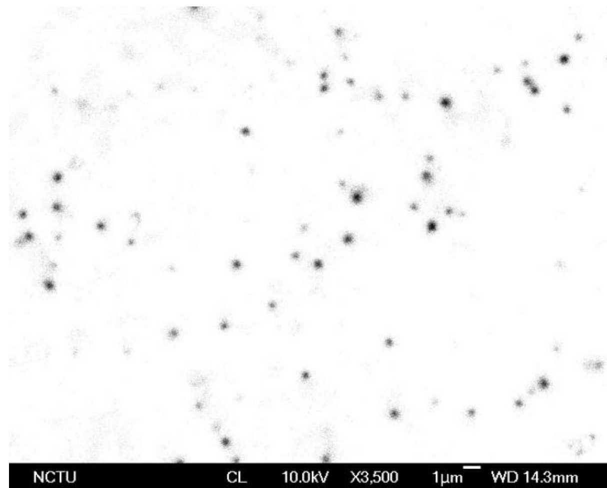

(b) Sample B

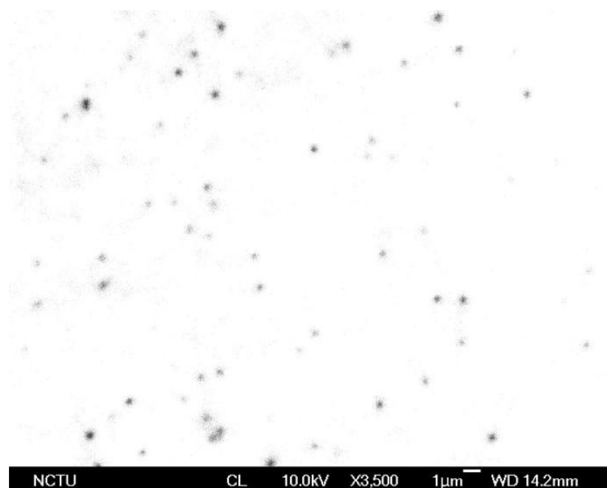

(c) Sample C

Figs. 4.9[(a)-(c)] Plane-view CL images of difference samples.

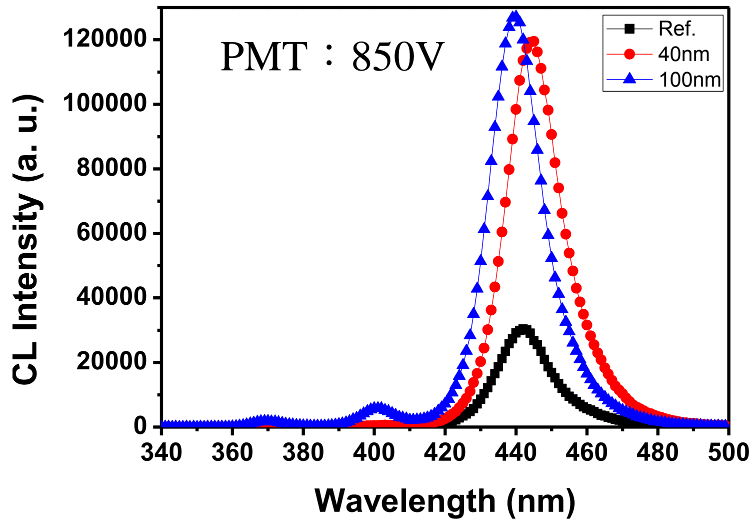

(a)

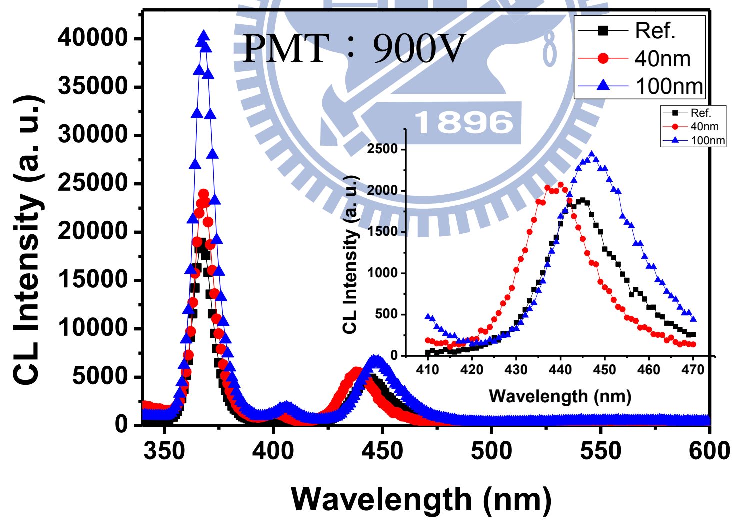

(b)

Figs. 4.10[(a)-(b)] CL spectrum of (a) plane-view and (b) cross section LED structure.

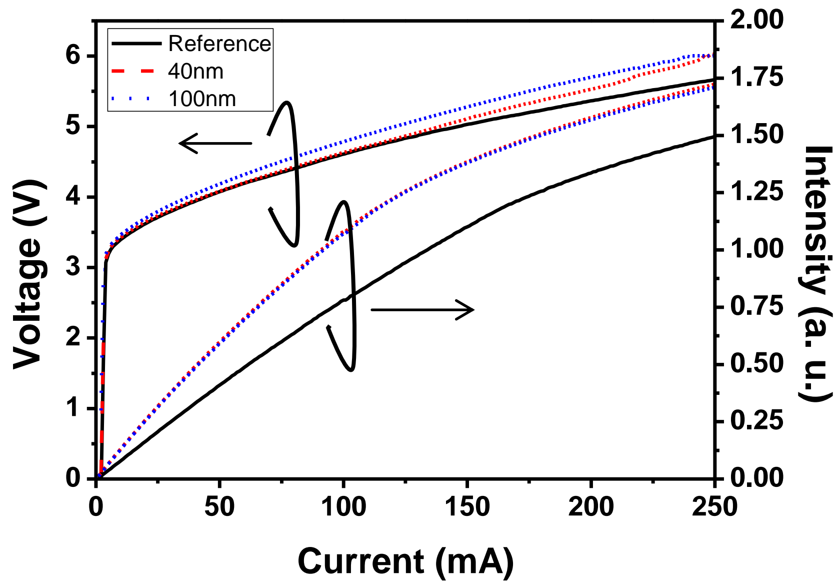

Fig. 4.11 L-I and V-I curve of DSP-LEDs and ref-LED.

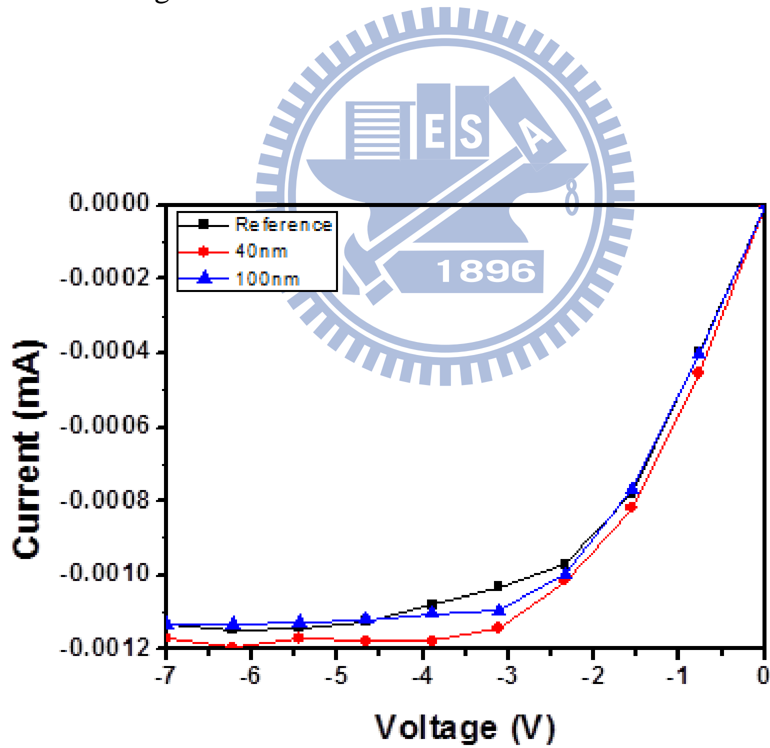

Fig. 4.12 Leakage current of DSP-LEDs and ref-LED under reverse bias.

4.4 Reference

[1] S.K. Hong*,1, B.J. Kim, H.S. Park, Y. Park, S.Y. Yoon, T.I. Kim, J. Cryst. Growth, 191 (1998).

[2] S. K. Hong, T. Yao, B. J. Kim, S. Y. Yoon, and T. I. Kim, *Appl. Phys. Lett.* 77, 82 (2000).

[3] L. Lu, Z. Y. Gao, B. Shen, F. J. Xu, S. Huang, Z. L. Miao, Y. Hao, Z. J. Yang, G. Y. Zhang, X. P. Zhang, J. Xu, and D. P. Yu, *J. Appl. Phys,* 104, 123525 (2008).

[4] T. Hino, S. Tomiya, T. Miyajima, K. Yanashima, S. Hashimoto, and M. Ikeda, Appl. Phys. Lett., 76, 3421 (2000)

[5] J. W. P. Hsu, M. J. Manfra, R. J. Molnar, B. Heying, and J. S. Speck, *Appl. Phys. Lett.* 81, 79 (2002)

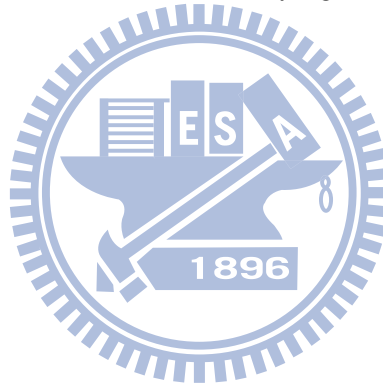

Chapter 5 Conclusion & Future work

In summary, we successfully simplify the process of defect selective passivation technique by choosing the GaN wafer with native pits and spin-coating silica nanospheres on GaN surface. This technique can effectively not only block the propagation of threading dislocations but also improve the crystal quality of GaN epilayer. Eventually, we use the GaN epilayer dealt with defect selective passivation technique to fabricate high efficient LED.

There are some further studies listed in the following:

1. Exploring additional chemical solution that is complementary to KOH in defect selective etching to increase the coverage rate of defect selective passivation. Same passivation process needs to be investigated before sending the wafer back to MOCVD for GaN epitaxial growth.
2. To measure the beam profile of LED at the operating current is the other further work. Try to change the size of nanospheres if the divergent angle of the LED is identified.